ACS OMEGA

http://pubs.acs.org/journal/acsodf

Article

Enhancing Sustainable Production of Fatty Acid Methyl Ester from Palm Oil Using Bio-Based Heterogeneous Catalyst: Process Simulation and Techno-Economic Analysis

Phonsan Saetiao, Napaphat Kongrit, Jakkrapong Jitjamnong,* Chatrawee Direksilp, Chin Kui Cheng, and Nonlapan Khantikulanon

Cite This: *ACS Omega* 2023, 8, 30598−30611

Read Online

ACCESS | Metrics & More | Article Recommendations | Supporting Information

ABSTRACT: A new sustainable solid carbon catalyst has been developed for biodiesel synthesis using pyrolytic coconut shell ash (CSA). The CSA support was loaded with various amounts of potassium carbonate (K_2CO_3), and response surface methodology with a central composite design was used to optimize the transesterification process. The best-performing catalyst was the 30 wt % K_2CO_3/CSA catalyst. The optimal conditions included a catalyst loading of 3.27 wt %, methanol:oil molar ratio of 9.98:1, reaction time of 74 min, and temperature of 65 °C, resulting in an obtained biodiesel yield of 97.14%. This catalyst was reusable for up to four cycles, but a reduction in the biodiesel yield was observed due to potassium ion leaching during the recovery process. A techno-economic analysis to assess the financial viability of the project revealed a net present value of 5.16 million USD for a project lifetime of 20 years, a payback period time of 2.49 years, and an internal rate of return of 44.2%. An environmental assessment to evaluate the impact of global warming potential from the production of biodiesel revealed a lower level of carbon dioxide emission (1401.86 ton/y) than in the conventional process (1784.6 ton/y).

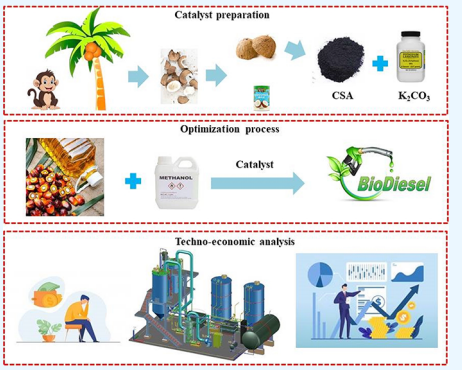

1. INTRODUCTION

The global reliance on petroleum as a predominant energy resource has engendered profound consequences for the environment, economy, and society. According to prevailing estimations, fossil fuels fulfill around 80% of the world's energy requirements, leaving a mere 20% sourced from renewable outlets.[1] The depletion of petroleum oil (nonrenewable) can lead to significant economic and environmental consequences.[2] The combustion of petroleum-based fuels releases harmful greenhouse gases (GHGs) and so contributes to global warming and climate change. However, recent developments have shown that there is hope for reducing our reliance on petroleum through the use of biodiesel. Biodiesel, composed of fatty acid methyl esters (FAMEs), possesses a multitude of advantages in contrast to conventional diesel fuel. For one, it reduces GHGs emissions and has a lower carbon footprint.[3] It also produces lower levels of toxic pollutants, such as sulfur oxides, benzene, carbon monoxide, carbon dioxide (CO_2), nitrogen oxides, and particulate matter.[4]

Biodiesel is typically produced by transesterification of oils or fats with a small primary alcohol in the presence of a catalyst. The choice of catalyst plays a critical role in the efficiency, selectivity, and cost-effectiveness of the biodiesel production process. Homogeneous catalysts can offer a higher selectivity and reactivity than heterogeneous catalysts, producing biodiesel with a high purity and yield, which makes them attractive for small-scale production. Homogeneous base catalysts, such as sodium hydroxide[5] or potassium hydroxide (KOH),[6] can be used to catalyze the transesterification reaction, and they typically exhibit higher activity than heterogeneous catalysts. However, homogeneous catalysts also have some drawbacks for biodiesel production. They can be more difficult to separate from the reaction mixture, leading to additional processing steps and costs.[7]

Consequently, the use of heterogeneous catalysts for biodiesel production has gained increasing attention in recent years due to their ease of handling and separation from the reaction mixture. They can be reused multiple times and are generally more stable than homogeneous catalysts. Various heterogeneous catalysts, such as metal oxides,[8−10] have been shown to be effective in catalyzing the transesterification reaction. Since they can be easily recovered and recycled, this reduces the overall cost of the biodiesel production process.[11,12]

Received: June 14, 2023
Accepted: August 1, 2023
Published: August 10, 2023

Among the various heterogeneous catalysts, biochar-derived catalysts have emerged as a promising option due to their low cost, high stability, and potential for waste valorization. Biochar is a carbon-rich material obtained by the hydrothermal carbonization of biomass. The physicochemical properties of biochar, such as its surface area, pore size distribution, and functional groups, can be tailored through different pyrolysis conditions, making it an attractive precursor for the synthesis of heterogeneous catalysts.[13]

Various activated biochars have shown promising potentials as catalysts in the production of biodiesel. Their effectiveness stems from their large surface area, increased pore size, and diverse functional groups. The presence of inorganics, such as sodium (Na), calcium (Ca), potassium (K), magnesium (Mg), and iron (Fe), has been found to play a crucial role in the catalytic properties of biochar.[14] In another study, biochar/calcium oxide (CaO)/potassium carbonate (K_2CO_3) was prepared from algal biochar and then used as a transesterification catalyst. The catalyst showed an excellent catalytic activity and reusability, with a conversion rate of 98.83% after five cycles of use.[15]

Techno-economic analysis (TEA) is an essential tool for evaluating the economic feasibility of an industrial process. By accounting for the material balance of various process streams, the TEA produces valuable simulation data. It is a valuable tool for companies looking to optimize their manufacturing processes and make informed decisions about the economic viability of their operations. By providing a comprehensive view of the costs and benefits of a process, TEA also includes a profitability analysis that examines the revenues generated by the main product and by-products.[16] Moreover, TEA can help businesses identify areas for improvement and make strategic investments in their operations. Furthermore, it can be used to assess the environmental impact of a process. This information can be used to identify opportunities for reducing the environmental impact and improving sustainability.[2]

A novel method to produce biodiesel from castor oil using a heterogeneous catalyst was recently developed through extensive optimization, while the TEA demonstrated that the process had the potential to generate substantial revenue, with total estimated revenue of 16,506,000 USD/y.[16] Furthermore, the payback period (PBP) for this process was relatively short at 2.88 y. One of the key factors that contributed to the economic viability of this process was the recycling of both the catalyst and methanol. Likewise, the potential of using marine macroalgae oil for biodiesel production was evaluated by TEA and revealed that the return on investment and internal rate of return (IRR) were 25.39 and 31.13%, respectively.[17] The plant PBP was estimated to be 3.94 y, and the net present value (NPV) was calculated to be approximately 14,053,000 USD/y.

Based on the above facts, this study developed a promising new catalyst system for the cost-effective and environmentally sustainable production of biodiesel. The catalyst was made from the pyrolysis of CS to form CS ash (CSA) as the support for different loading levels of the alkaline (calcined K_2CO_3) catalyst. This innovative catalyst was optimized for efficient biodiesel production through process optimization using response surface methodology (RSM) to determine the ideal process conditions for biodiesel production, including the methanol:palm-oil molar ratio (3.95:1−14.05:1), catalyst concentration (2.32−5.68 wt %), and reaction time (39.55−140.45 min). The process flow diagram of the biodiesel production plant was designed using the Aspen Plus software. The sensitivity analysis on the raw materials purchase cost and biodiesel price was analyzed to determine the most cost-effective conditions for production.

2. MATERIALS AND METHODS

2.1. Materials. The CS, as agricultural waste, were collected from households in Songkhla, Thailand, and used to create the CSA as the catalyst support. Palm oil, purchased from a local supermarket in Thailand, with the previously reported physicochemical properties,[18] was used along with methanol (99.5% purity) to synthesize the biodiesel. KOH (85% purity) was used to pretreat the CSA. These were all from RCI Labscan, Ltd., Ireland. The AR grade *n*-heptane, used as a solvent for the gas chromatography (GC) analysis, was purchased from Fisher Scientific in England, while K_2CO_3 (99% purity), used as an alkaline metal, was obtained from Ajax Finechem Pty., Ltd., in Australia.

2.2. Catalyst Preparation. The CS were manually cut into small pieces and washed thoroughly with distilled water in order to remove any impurities or dust. They were then dried in an oven at 80 °C overnight to complete dryness, ground into a fine powder, and passed through a sieve with an 18-mesh size to yield a fine CSA. The fine CSA was calcined at 600 °C for 2 h with a heating rate of 10 °C/min and then chemically activated by suspending it in 2 M KOH solution, as previously reported.[19] The suspension was then filtered, washed repeatedly with distilled water until the eluate reached pH 7.0, and dried at 105 °C overnight.

The activated CSA support (hereafter called CSA) was impregnated with K_2CO_3 via the wet impregnation method to achieve different loading levels of 25−35 wt % at 25 °C. To achieve a 25 wt % loading, 2.5 g of K_2CO_3 was dissolved in distilled water and mixed with 7.5 g of CSA, stirred for 4 h to ensure proper impregnation of the catalyst, and aged for another 24 h. The catalyst was then dried overnight at 105 °C in an oven to remove any remaining moisture and calcined at 600 °C for 4 h under atmospheric pressure at a ramp rate of 10 °C/min. The resulting catalyst was then stored in a desiccator to prevent moisture and CO_2 interaction with the catalyst. The catalyst was named αK/CSA, where α represents the K_2CO_3 concentration level used in the impregnation.

2.3. Catalyst Characterization. The structure and chemical composition of the catalyst was evaluated using powder X-ray diffractometry (XRD) analysis. The solid powder sample was subjected to XRD using Cu Kα radiation (λ = 0.15405 nm) with a 2.2 kW Cu anode and fine focus ceramic X-ray tube. The XRD analysis was performed at 25 °C within a 2θ range between 15 and 75°, a scanning speed of 5°/min, and a scan step of 0.02°.

The basic strength of the prepared catalyst was evaluated using the Hammett indicator method to determine its total basicity in a solution of 0.01 M benzoic acid in anhydrous methanol. The following indicators were employed: bromothymol blue (with an H_ value of 7.2), phenolphthalein (with an H_ value of 9.8), 2,4-dinitroaniline (with an H_ value of 15.0), and 4-nitroaniline (with an H_ value of 18.4).

To assess the surface characteristics of the catalyst, the nitrogen adsorption−desorption profile was analyzed using the Brunauer−Emmett−Teller (BET) method over a pressure range (P/P_0) of 0.02−0.2 starting at a temperature of −196 °C. The volatile species that were adsorbed onto the surface of the catalyst were removed through a vacuum outgassing process overnight at a temperature of 250 °C.

https://doi.org/10.1021/acsomega.3c04209
ACS Omega 2023, 8, 30598−30611

The functional groups of the catalyst were conducted by Fourier transform infrared spectroscopy (FTIR) analysis. The solid samples were compressed with KBr powder into disks. The FTIR spectrum was then collected using a Perkin-Elmer spectrometer, operating in the wavenumber range of 4000−650 cm^{-1}. The 32 scans at a 4 cm^{-1} resolution were performed in the absorbance mode, which enabled a high-quality spectrum to be obtained.

Investigation of the surface morphology and elemental distribution of the catalyst was performed using scanning electron microscopy−energy dispersive spectroscopy (SEM-EDS) using the Oxford Aztec model at a magnification of 1000 times and an accelerating voltage of 10 kV. Prior to the SEM-EDS analysis, the specimen was coated with a thin layer of gold.

The catalyst chemical composition, specifically the O 1s and K 2p levels, were analyzed using X-ray spectroscopy (XPS). The XPS spectra were obtained using monochromatized Al Kα radiation (1486.6 eV) with a Kratos Axis Ultra DLD. Analyzer pass energies of 160 and 40 eV were used for the survey and high-resolution scans, respectively. To reference the binding energy (BE) scale, the peak maximum in the C 1s spectrum was set to 284.8 eV.

2.4. Process Optimization for Biodiesel Production. In this study, the optimization of biodiesel yield was conducted using a CCD with RSM, since CCD is a suitable experimental design for conducting sequence experiments with a small number of design points. The design variables considered in this study were the catalyst loading level, methanol:oil molar ratio, and reaction time, while the response value was the biodiesel yield (Table S1). To conduct the experimental design and analysis, the Design Expert version 13 software trials from Stat-Ease Inc. was employed. A total of 20 experimental runs were carried out (total run = $2^y + 2y + 6$, where y is the number of independent factors and 6 is the number of replicate points at the central point). To establish the reaction factors, a second quadratic model was utilized, as represented in eq 1.

$$Y = \beta_0 + \sum_{i=1}^{3} \beta_i X_i + \sum_{i=1}^{3} \beta_{ii} X_i^2 + \sum_{i=1}^{3} \sum_{j=2}^{3} \beta_{ij} X_i X_j + \varepsilon \quad (1)$$

This model included parameters for constant (β_0), linear (β_i), quadratic (β_{ii}), and interaction coefficients (β_{ij}), as well as random error (ε). These parameters were determined through regression analysis and analysis of variance (ANOVA). The established model was then used to determine the optimal conditions for maximizing the biodiesel yield.

2.5. Biodiesel Production from Palm Oil and Methanol. The palm oil was placed in a 500 mL three-neck round-bottom flask, equipped with a condenser, thermometer, and magnetic stirrer. It was then heated and stirred at 65 °C on a hotplate and stirrer, allowing for the palm oil to become less viscous and more reactive. Next, the amount of methanol to give the desired palm oil:methanol molar ratio (ranging from 3.95:1 to 14.05:1) and catalyst mixture (2.32−5.68 wt %) was prepared and added to the preheated oil with stirring at 500 rpm. After the predetermined reaction time (ranging from 39.55−140.45 min), the catalyst was removed from the mixture by filtration. The resulting solution was allowed to phase separate in a separating funnel, with the glycerol in the lower layer being decanted. The upper phase containing the biodiesel was washed with hot distilled water until the water remained neutral (pH 7.0) to ensure the purity of the biodiesel. The obtained biodiesel was stored in a glass bottle with sodium sulfate anhydrous to remove any residual water. The biodiesel yield was calculated using eq 2:

$$\text{biodiesel yield (\%)} = \frac{\text{weight of biodiesel produced}}{\text{weight of starting palm oil used}} \quad (2)$$

The reusability of the catalyst was evaluated in successive transesterification reactions. After each reaction, the spent catalyst was thoroughly washed with hexane to remove any residue and then dried overnight in an oven at 105 °C to prepare for the next run.

2.6. Biodiesel Analysis. The FAME composition of the obtained biodiesel was investigated using GC equipped with a flame ionization detector. A DB-WAX fused-silica capillary column was used as the column for the GC analysis. The biodiesel sample was injected into the GC system with a helium carrier gas flow rate of 70 mL/min, injector temperature of 200 °C, split ratio of 75:1, detector temperature of 230 °C, and oven temperature of 130 °C. The GC oven was heated gradually to 230 °C and held for 15 min, resulting in a total run time of 62.5 min. The FAME composition was analyzed in comparison with the mass spectra of the FAME standard mixture and retention time.

2.7. Process Design of Biodiesel Production. Triolein ($C_{57}H_{98}O_6$) and methyl oleate ($C_{19}H_{36}O_2$) were utilized as model compounds to represent palm oil and the product of transesterification reactions, respectively. Aspen Plus V11 and Economic Evaluator in Aspen Plus were employed to conduct the simulation work and cost estimation evaluations. The nonrandom two liquid (NRTL) model was selected as the thermodynamic model, predicting the vapor−liquid equilibrium (VLE) and liquid−liquid equilibrium (LLE) through binary interaction parameters from a previous work.[20]

2.8. Biodiesel Production: TEA. This study employed a case study approach to analyze the techno-economic performance of a biodiesel production plant with a capacity of 1050 kg/h of oil feed. The biodiesel production plant used palm oil as the feedstock and employed transesterification with methanol as the conversion process. An evaluation of the costs and benefits was conducted to estimate the equipment size using the Aspen Process Economic Analyzer. This tool facilitated the transfer of the Aspen Plus flowchart unit operations to the device cost model, providing a projected cost of purchased equipment and the total direct cost (TDC) from the supplier. The study considered various factors, such as capital investment, operating cost, revenue, NPV, IRR, PBP, and sensitivity analysis. The operating time for the biodiesel production plant was estimated to be 8400 h/y, with a project evaluation time of 20 y. The production plant operated for 50 weeks/y, with 5 shifts/week/person, and 3 shifts/d. This duration accounts for the deduction of sick and vacation days from the total of 52 weeks in a year. The number of operators required (N_{OL}) for the plant was estimated using eq 3, which takes into account the total number of particulate (P) and nonparticulate (N_{np}) handling unit operations.[21] This can help improve the production efficiency, reduce labor costs, and improve decision-making processes.

$$N_{OL} = (6.29 + 31.7P^2 + 0.23N_{np})^{0.5} \quad (3)$$

The NPV is a powerful tool for evaluating the worth of a project, providing decision-makers with valuable insights into

https://doi.org/10.1021/acsomega.3c04209
ACS Omega 2023, 8, 30598−30611

its financial feasibility. A positive NPV indicates that the project is expected to generate profits, while a negative NPV suggests that the project may not be financially viable. The NPV is calculated based on the cash flows of a project, which are then discounted using a discount rate to reflect the time value of money. The formula for calculating the NPV is shown in eq 4:

$$\mathrm{NPV} = \sum_{t=0}^{n} \frac{R_t}{(1+\mathrm{i})^t} \tag{4}$$

where t represents the year of operation or number of periods, R_t represents the cash inflow minus cash outflow over period t, and i represents the discount rate. The discount rate is typically based on the capital cost or the required rate of return for similar investments. A higher discount rate will result in a lower NPV, as the future cash flows are discounted at a higher rate.

Another economic measure, the PBP is a popular financial metric used by companies to assess the feasibility of their investment projects. It is the length of time required for an investment to recover its initial cost and is calculated by dividing the initial investment by the annual cash inflows generated by the investment, as shown in eq 5.

$$\mathrm{PBP} = \frac{\text{cost in investment}}{\text{annual net cash flow}} \tag{5}$$

On the other hand, the IRR is a widely used financial metric in investment analysis. It is a financial risk indicator that helps investors assesses the profitability of an investment over a specified period of time. The IRR is the discount rate at which the NPV of an investment equals zero, as shown in eq 6.

$$\mathrm{NPV} = 0 = \sum_{t=1}^{n} \frac{C_t}{(1+\mathrm{IRR})} - C_0 \tag{6}$$

The variable t in the equation represents the number of time periods over which the cash flows are generated. The net cash inflow generated by the investment project during each period is denoted by C_t, and the total initial investment cost is denoted by C_0.

Biodiesel production involves various costs, including those of raw materials,[22−26] products,[27,28] and utilities.[29,30] These costs can vary, depending on the availability and price of the raw materials in the market (Table 1). Utility costs are another important aspect of biodiesel production. These costs include the cost of electricity, process steam, and cooling. Heating of chemical reactors for the reactants (palm oil and methanol) is one of the primary utility costs for biodiesel production. Additionally, for a biodiesel refinery, heating of chemical reactors for distillation towers is also a significant utility cost. The data, encompassing the mass balance obtained from Aspen Plus, has been quantified in a rigorous manner.[31−33]

2.8.1. Total Capital Investment (TCI). An overview of the TCI assumptions based on previous work-based calculations by Peters et al. in 2003[34] is shown in Table 2. The TCI was divided into two main categories: fixed capital investment (FCI) and working capital investment (WCI). The FCI was further sub-divided into direct costs and indirect costs.

2.8.2. Total Product Cost (TPC). The TPC of biodiesel production is the sum of all costs incurred in the process of converting palm oil into biodiesel. An overview of the TPC assumptions developed based on the previously established principles by Peters et al., 2003,[34] is represented in Table 3.

Table 1. Economic Assumptions for the Cost of Raw Materials, Products, and Utilities

item	cost	CO_2 emission amount (kg CO_2/GJ)	reference
raw materials			
palm oil	0.255 USD/kg		22
methanol	0.23 USD/kg		23
K_2CO_3	1.30 USD/kg		24
KOH	2.20 USD/kg		25
water	0.0061 USD/kg		26
products			
biodiesel	1.0 USD/kg		27
glycerol	0.265 USD/kg		28
utilities			
steam (2 bar, 120 °C)	10.69 (USD/GJ)	66.68	29
low pressure steam (6 bar, 160 °C)	11.80 (USD/GJ)	72.86	29
medium pressure steam (11 bar, 184 °C)	13.28 (USD/GJ)	76.60	29
high pressure steam (42 bar, 254 °C)	15.73 (USD/GJ)	91.14	29
cooling water	0.354 (USD/GJ)		29
chilled water	4.43 (USD/GJ)		29
electricity	0.06 (USD/kWh)	120.06	30

Table 2. Total Capital Investment (TCI) Assumptions

cost parameter	percentage
total direct cost (TDC)	
purchased equipment cost (PEC)	
land	8% of PEC
buildings, process, and auxiliary	10% of PEC
equipment installation and painting	25% of PEC
instrumentation and controls (installed)	10% of PEC
piping (installed)	10% of PEC
electrical system (installed)	10% of PEC
service facilities and yard improvements	40% of PEC
total indirect cost (TIC)	
engineering and supervision	5% of TDC
legal expense	1% of FCI
construction expense and constructor's free	10% of FCI
contingency charges	5% of FCI
fixed capital investment (FCI)	TDC + TIC
working capital investment (WCI)	5% of FCI
total capital investment (TCI)	FCI + WCI

The TPC of biodiesel production can be broken down into several components. These components include direct production costs, fixed charges, plant overhead, and general expenses.

2.9. Environmental Analysis. Climate change is a significant and urgent issue that requires immediate attention from individuals, communities, and governments around the world. The concept of carbon footprint refers to the total amount of GHGs, mainly CO_2, released into the atmosphere due to human activities. It is usually measured in terms of mass or weight of CO_2 equivalent produced per unit of product or service.[35] Aspen Plus process simulation software was used to estimate the CO_2 emissions.

https://doi.org/10.1021/acsomega.3c04209
ACS Omega 2023, 8, 30598−30611

Table 3. Total Product Cost (TPC) Assumptions

description	percentage
direct production	
raw materials	C_{RM}
utilities	C_{UT}
operating labor	C_{OL}
operating supplies	0.5% of FCI
maintenance and repairs	2% of FCI
fixed charges	
insurance	0.4% of FCI
local taxes	1% of FCI
plant overhead	5% of TPC
cost of manufacturing (COM)	direct production + fixed charges + plant overhead
general expenses (GE)	
research and development	5% of TPC
distribution and marketing	2% of TPC
administrative	2% of TPC
total product cost (TPC)	COM + GE

3. RESULTS AND DISCUSSION

3.1. Screening of the Catalyst. The CSA support alone was ineffective in promoting the reaction, but when K_2CO_3 was loaded onto the CSA, a high yield of biodiesel was obtained. This suggests that supporting potassium compounds on the CSA was essential for generating catalytic activity in the transesterification reaction. Interestingly, the synthesized catalyst loaded with 30 wt % K_2CO_3 exhibited the highest biodiesel yield (96.4%). However, increasing the K_2CO_3 loading level above 30 wt % did not significantly improve the biodiesel yield with only a slight numerical increase from 96.4 to 96.5%. This was likely due to the excessive potassium compounds covering the active sites.[36] Thus, the 30 K/CSA catalyst was deemed to be the most promising for further study in the transesterification of palm oil/ methanol to biodiesel, and its properties were analyzed in more detail.

3.2.1 XRD Analysis. The XRD analysis of the CSA revealed broad peaks in the range of 20 to 30° and a broad diffraction peak at a 2θ of 35−50°, which indicates the amorphous nature of the cellulose network, consistent with the existing literature[11] (Figure S1). Additionally, two peaks at 2θ values of 26.58 and 43.14° were observed, suggesting the presence of graphitized carbon[15,36] However, the CSA modified with various concentrations of K_2CO_3 exhibited more peaks in their XRD patterns. Specifically, the peaks at a 2θ of 28.64, 38.56, 40.44, and 57.14° were attributed to the presence of tetragonal potassium, while the peaks at 2θ values of 25.73, 41.31, 42.41, and 45.01° were assigned to the presence of K_2O,[37] indicating its role as the primary component in the catalyst. The modification of the CSA with K_2CO_3 showed alterations in the range and intensity of the peaks, indicating the successful incorporation of K_2CO_3 into the composite structure and the creation of the target catalyst, which may enhance the catalytic activity of the catalyst.

3.2.2 Basic Strength. The basic strength (H_) and basicity of the CSA modified with different K_2CO_3 levels was evaluated using the Hammett indicator and titration method, respectively. The titration method for determining basicity involves adding standardized acidic solution to the sample, causing a neutralization reaction with the basic components. The endpoint, indicated by a color change, represents the stoichiometric balance between acid and base. Basicity is quantified by measuring the volume of acidic solution needed to reach this endpoint. The unmodified CSA support exhibited a low basic strength and basicity, resulting in no catalytic activity (no FAME yield) (Table S2). However, loading K_2CO_3 onto the CSA (from 25 to 35 wt %) induced a marked increase in the basic strength (range of 9.8−15.0) and total basicity (5.20−7.10 mmol/g). The catalytic activity of the synthesized catalysts was closely linked to their basic strengths and basicity, with higher levels resulting in higher biodiesel yields.

According to the XRD results, the total basicity of the catalyst was primarily influenced by the presence of K_2O and K_2CO_3 on its surface. However, increasing the K_2CO_3 loading beyond 30 wt % did not lead to a significant improvement in the total basicity, increasing only slightly numerically from 6.83 to 7.10 mmol/g. This was due to the excessive potassium compounds covering the surface basic sites, making them inaccessible to incoming reactants.[36]

3.2.3 BET Surface Area (S_{BET}) Analysis. The BET isothermal analysis was used to determine the S_{BET} of the CSA and 30 K/CSA heterogeneous catalyst samples. The S_{BET} of the CSA support (503.52 m^2/g) was higher than that of the 30 K/CSA catalyst (140.31 m^2/g), suggesting that K_2CO_3 effected the catalyst structure. The reduction in the S_{BET} of the 30 K/CSA catalyst compared to the CSA support may be due to the agglomeration of K_2O and/ or K_2CO_3 particles on the CSA surface.[11,15] Despite this reduction, changes in the surface features confirmed the successful synthesis of the 30 K/CSA catalyst.

3.2.4 Functional Groups: FTIR Analysis. The FTIR spectra revealed bands above 3624.83 and 1665.48−1675.76 cm^{-1} due to hydroxyl groups, which reflects the presence of moisture adsorbed onto the surface of the prepared catalyst[36,38] (Figure S2). In the FTIR analysis of CSA, distinct peaks were observed at 2973.70 and 2886.50 cm^{-1}, which were attributed to C−H stretching vibrations. These peaks are often seen in the IR spectra of biomass and biochar.[39] Additionally, a peak at around 1058.06−1077.23 cm^{-1} was observed, which corresponds to single bond C−O.[40] Interestingly, the FTIR spectra of both the CSA and 30 K/CSA catalyst exhibited peaks at 865−876 cm^{-1}, indicating the presence of carbonate groups.[36,41] This was due to the reaction of CO_2 in the air with alkali during the preparation of the samples, indicating the formation of a small amount of K_2O or K_2CO_3. Notably, the 30 K/CSA catalyst showed additional peaks at 1447.36, 1380.50, and 704.26 cm^{-1}, which were ascribed to carbonate species of K_2O loaded onto the support. These peaks were caused by thermal degradation during calcination.[36,39,42]

3.2.5 Surface Morphology: SEM Analysis. The CSA powder exhibited a smooth and wrinkled structure with a few voids (Figure S3). On the other hand, the 30 K/CSA powder displayed wrinkled and agglomerated particles on the surface. The formation of agglomerate particles in the 30 K/CSA catalyst is mainly attributed to the thermal decomposition of K_2CO_3 to K_2O during the calcination step. The surface of the 30 K/CSA catalyst displayed an agglomerated texture, which was discovered to be the result of the volatilization of organic materials during the calcination process. As a result, gaseous CO_2 and water molecules were released from the surface, leaving behind a powder composed mainly of K_2O. Thus, the 30 K/CSA catalyst, which is predominantly composed of K_2O, has been identified as a potential candidate

https://doi.org/10.1021/acsomega.3c04209
ACS Omega 2023, 8, 30598−30611

for use as a heterogeneous base catalyst in the biodiesel production process.

The EDS analysis results showed that the CSA consisted mainly of carbon (C), oxygen (O), and K elements with a small amount of K_2O, while the 30 K/CS catalyst contained C, O, K, and silicon (Si) elements (Figure S4). Of particular interest was the significant increase in the potassium content of the 30 K/CSA catalyst, which went from 1.8 to 25.4 wt %. This finding suggests that the loaded K_2CO_3 was well distributed over the CSA, which is essential for effective catalytic activity. The increased potassium content suggests that the catalyst may be effective in catalyzing reactions that require high potassium levels.

3.2.6 XPS Analysis. The XPS analysis revealed that the CSA catalyst was composed primarily of C (74.92%), K (18.87%), and O (6.21%) (Figure S5). The carbon peaks at a BE of 284.00 eV corresponded to C−C/C=C bonds.[43] The K 2p peaks at BE values of 292.97 and 293.66 eV suggested the presence of potassium in the form of K_2O or K_2CO_3. For the 30 K/CSA catalyst (Figure S5), the XPS analysis revealed a different surface composition. Carbon was still the most abundant element, followed by O and K. The single O 1s peak produced at a BE of 529 eV confirmed that all the oxygen atoms were present in the form of metal carbonate or oxide. The K 2p peaks at a BE of 292.76 and 295.49 eV also confirmed the presence of potassium in the form of K_2CO_3 or K_2O. Thus, the XPS analysis provided concrete evidence of the successful loading of K_2CO_3 onto the CSA, corroborating the findings of the EDS analysis, which could have important implications for catalyzing chemical reactions.

3.3 Process Optimization: RSM Statistical Analysis. The design expert software (version 13 trials) was used to optimize the biodiesel yield. The experiment was conducted with 20 factorial points, each with three process parameters and five coded levels per parameter. Based on the CCD, the resulting experimental biodiesel yields are shown in Table 4, with a maximum obtained yield of 96.90%. Regression analysis was then performed using the experimental yield data, and a quadratic fit was determined as the best fit (Table 5). The ANOVA based on the RSM regression model coefficient values revealed an observed *F*-value of 18.43 (Table 6). Corresponding *p*-values were less than 0.05, indicating the significance of the model. Significance of the regression coefficient terms was considered when their respective *p*-values were less than 0.05.[1] The findings revealed that the linear effect of the methanol:oil molar ratio (B), the interaction between the catalyst loading and methanol:oil molar ratio (AB), the interaction between the methanol:oil molar ratio and reaction time (BC), and the second order effect of the methanol:oil molar ratio (B^2) were significant predictors of the model's outcome.

Table 4. Experimental and Predicted FAME Yield Values from the Response Surface Analysis

run	catalyst loading (wt %) (*A*)	methanol:oil molar ratio (*B*)	reaction time (min) (*C*)	actual FAME yield (%)	predicted FAME yield (%)
1	4	3.95:1	90	86.81	85.09
2	4	9:1	90	96.90	96.39
3	3	12:1	60	96.62	96.35
4	4	9:1	90	96.65	96.39
5	4	9:1	90	96.20	96.39
6	5.68	9:1	90	96.05	95.31
7	5	12:1	60	93.97	93.17
8	4	9:1	90	96.10	96.39
9	5	12:1	120	91.15	91.44
10	3	6:1	120	89.95	91.06
11	4	14.05:1	90	88.67	89.94
12	3	6:1	60	89.04	89.06
13	5	6:1	120	92.38	92.96
14	4	9:1	140.45	95.67	95.30
15	4	9:1	39.55	95.13	95.06
16	4	9:1	90	96.25	96.39
17	5	6:1	60	90.25	91.67
18	2.32	9:1	90	96.08	96.38
19	3	12:1	120	96.45	95.34
20	4	9:1	90	96.15	96.39

In the past, it was commonly believed that a high R^2 value indicated the best fit for a model. However, it was later discovered that this may not always be the case. Therefore, as the adjusted coefficient of determination (adj. R^2) was introduced to better evaluate a model's fitness while considering the predictor variables.[44] In this study, the R^2 and adj. R^2 values were determined to be 0.9431 and 0.8920, respectively. Furthermore, the adequate precision was found to be 14.788, which surpassed the desired value of greater than 4. These findings suggest that the model created in this study could be utilized for navigating the design space. The relationship between the independent variables and the response was modeled using a second-order polynomial equation, where the predicted FAME yield was calculated using eq 7:

$$\text{FAME yield} = 96.44 - 0.3193A + 1.44B + 0.0702C - 1.45AB - 0.1787AC - 0.7537BC - 0.2093A^2 - 0.315B^2 - 0.4444C^2 \quad (7)$$

where *A* is the catalyst loading level (wt %), *B* is the methanol:oil molar ratio, and *C* is the reaction time (min).

Assessing the accuracy of a regression model is a crucial step in predicting outcomes based on changes in independent variables. In this study, the parity plot and three diagnostic plots were used to evaluate the accuracy of the regression model that predicted the FAME yield based on variations in the catalyst loading level, methanol:oil molar ratio, and reaction time. The parity plot (Figure S6) shows that the predicted FAME yield closely aligned with the actual FAME yield. The data points cluster closely around the regression line, confirming that the predicted FAME yields accurately reflect the actual FAME yield in response to changes in the independent variables. The residuals plots, which are the differences between the actual and predicted values for each experimental point, were used to test the ANOVA assumption. The plot of the predicted FAME yield with respect to internally studentized residuals revealed that the residuals were randomly scattered (Figure S6), indicating that although the predicted observations deviated slightly from the actual observations, it was not significant.[45] This plot also validated the normality of the data. A plot of the internally studentized residuals versus the normal probability mostly followed a straight line (Figure S6), indicating that the residuals were normally distributed. The plot of the experimental run with residuals with respect to internally studentized residuals (Figure S6) shows that the standardized residuals satisfy the ANOVA assumption by lying within the interval of ±3,[46] and

https://doi.org/10.1021/acsomega.3c04209
ACS Omega 2023, 8, 30598−30611

Table 5. Fit Summary Statistics for the Model Prediction[a]

source	sum of squares	df	mean square	*F*-value	*p*-value	remark
mean vs total	1.761×10^5	1	1.761×10^5			
linear	29.87	3	9.96	0.899	0.4628	
2Fl	21.59	3	7.20	0.6019	0.6252	
quadratic	143.68	3	47.89	40.71	<0.0001	suggested
cubic	10.52	4	2.63	12.67	0.0044	
residual	1.25	6	0.2076			
total	1.763×10^5	20	8816.01			

[a]df is the degree of freedom.

Table 6. ANOVA Results for the Quadratic Unreduced Model for Biodiesel Production Using the 30 K/CSA Catalyst[a]

source	sum of squares	df	mean square	*F*-value	*p*-value	remark
model	195.14	9	21.68	18.43	<0.0001	significant
A, catalyst loading	1.39	1	1.39	1.18	0.3022	NS
B, methanol:oil molar ratio	28.41	1	28.41	24.15	0.0006	significant
C, reaction time	0.0672	1	0.0672	0.0571	0.8159	NS
AB	16.79	1	16.79	14.27	0.0036	significant
AC	0.2556	1	0.2556	0.2173	0.6511	NS
BC	4.55	1	4.55	3.86	0.0777	NS
A^2	0.6310	1	0.6310	0.5363	0.4808	NS
B^2	143.23	1	143.23	121.74	<0.0001	significant
C^2	2.85	1	2.85	2.42	0.1509	NS

[a]df is the degree of freedom; NS is not significant.

so the fitted model accurately approximates all the data without significant errors.

Perturbation plots were used to analyze the effect of the process variables on the obtained biodiesel yield (Figure S7). The plots allowed assessment of the impact of different factors at a specific point in the plan space by changing just one factor while keeping the others constant.[44] The methanol:oil molar ratio (*B*) was found to be the most significant factor affecting the biodiesel yield, where lower to middle values had a more significant impact on the yield than intermediary and higher levels. This suggests that careful consideration should be given to the oil:methanol molar ratio when attempting to optimize the yield. Catalyst loading (*A*) and reaction time (*C*) were also found to have a noticeable effect on the biodiesel yield, although not as significant as the methanol:oil molar ratio. These findings were also supported by the ANOVA analysis (Table 6), which showed similarities to the perturbation plot in terms of the factors with the most prominent effect on yield.

3.4 Interaction Effect of Process Parameters on the Biodiesel Yield: RSM Approach. In this study, the 30 K/CSA catalyst was used to produce biodiesel from palm oil and methanol. The Design Expert version 13 software was employed to conduct a response surface analysis, which involved creating contour and three-dimensional plots to identify the interaction between the operational factors and determine the optimal conditions for maximum biodiesel yield. The results of the study showed a quadratic model when one of the three variables was fixed.

3.4.1 Effect of Catalyst Loading and Methanol:Oil Molar Ratio on the FAME Yield. The effect of the catalyst loading level and methanol:oil molar ratio on the obtained FAME yield is illustrated in Figure 1a,b. When maintaining a constant reaction time of 90 min, increasing the methanol:oil molar ratio from 3.95:1 to 9:1 at a catalyst concentration of 4 wt % led to a significant enhancement in the FAME yield from 86.81 to 96.15%. This increase in yield is due to the excess of methanol molecules that act as a driving force for the reaction and help maintain the reaction equilibrium. However, increasing the methanol:oil molar ratio to 14.05:1 at a catalyst concentration of 4 wt % caused a slight reduction in the FAME yield to 88.67%, which was due to the dilution of solution mixtures and flooding of the active-sites of the heterogeneous catalyst that then decreases the interactions and slows down the reaction rate. Additionally, excess methanol can lead to the hydrolysis of the produced biodiesel, resulting in the formation of soaps and reducing the biodiesel yield.[47,48] Thus, the methanol:oil molar ratio is an essential parameter in determining the FAME yield in accordance with the *F*-value result.

On the other hand, there was no improvement in the FAME yield when the catalyst concentration was further increased from 2.32 to 5.68 wt % while maintaining a constant reaction time of 90 min and a methanol:oil molar ratio of 9:1. This may be because the catalyst was already saturated at the lower concentration of 2.32 wt %, and so increasing the catalyst concentration further did not have any effect on the reaction. Based on the ANOVA results, the effect of the catalyst loading was found to be insignificant over the tested range. This is in accordance with the earlier published work on the synthesis of biodiesel from a waste *Musa paradisiaca* plant derived catalyst, where increasing the catalyst concentration from 5 to 9 wt % did not result in a significant decline, nor did it lead to a further increase in the biodiesel yield.[47]

3.4.2 Effect of Catalyst Loading and Transesterification Reaction Time on the FAME Yield. A contour plot and surface plot showing the relationship between catalyst loading and reaction time on the obtained FAME yield at a constant methanol:oil molar ratio of 9:1 is shown in Figure 1c,d. According to the plot, the FAME yield initially increased as the reaction time increased from 39.55 to 90 min, which could be attributed to better mixing and a higher reaction rate at longer reaction times. However, when the reaction time was further

https://doi.org/10.1021/acsomega.3c04209
ACS Omega 2023, 8, 30598−30611

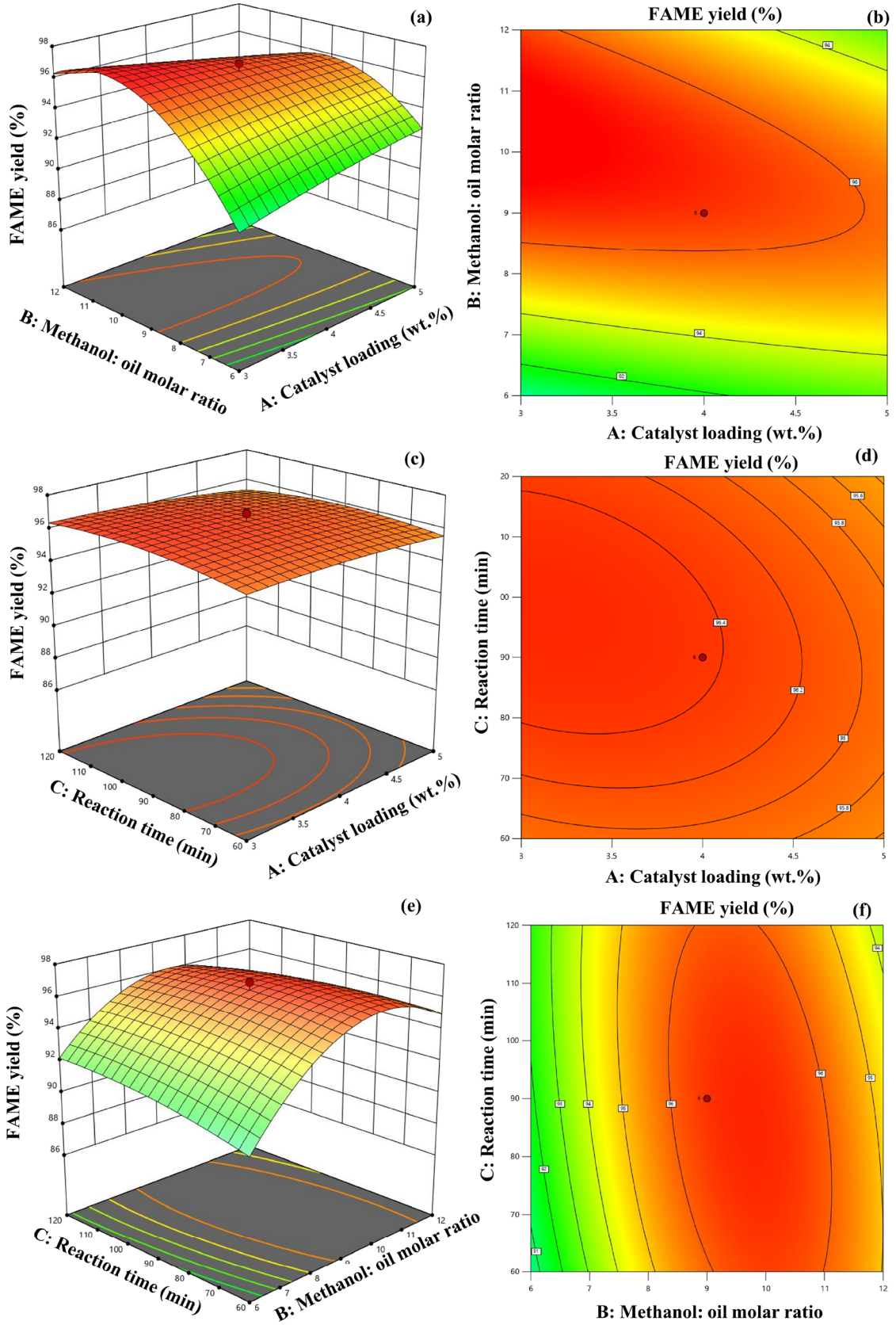

Figure 1. Surface response and contour plots showing the predicted values of the FAME yield: the interaction effects of the (a, b) catalyst loading and methanol:oil molar ratio, (c, d) catalyst loading and reaction time, and (e, f) reaction time and methanol:oil molar ratio.

increased to 140.45 min, the FAME yield decreased due to the reversible reaction between palm oil molecules and methoxide. The reaction had reached equilibrium, which resulted in a decreased yield of biodiesel.[11,47] Interestingly, no improvement

https://doi.org/10.1021/acsomega.3c04209
ACS Omega 2023, 8, 30598−30611

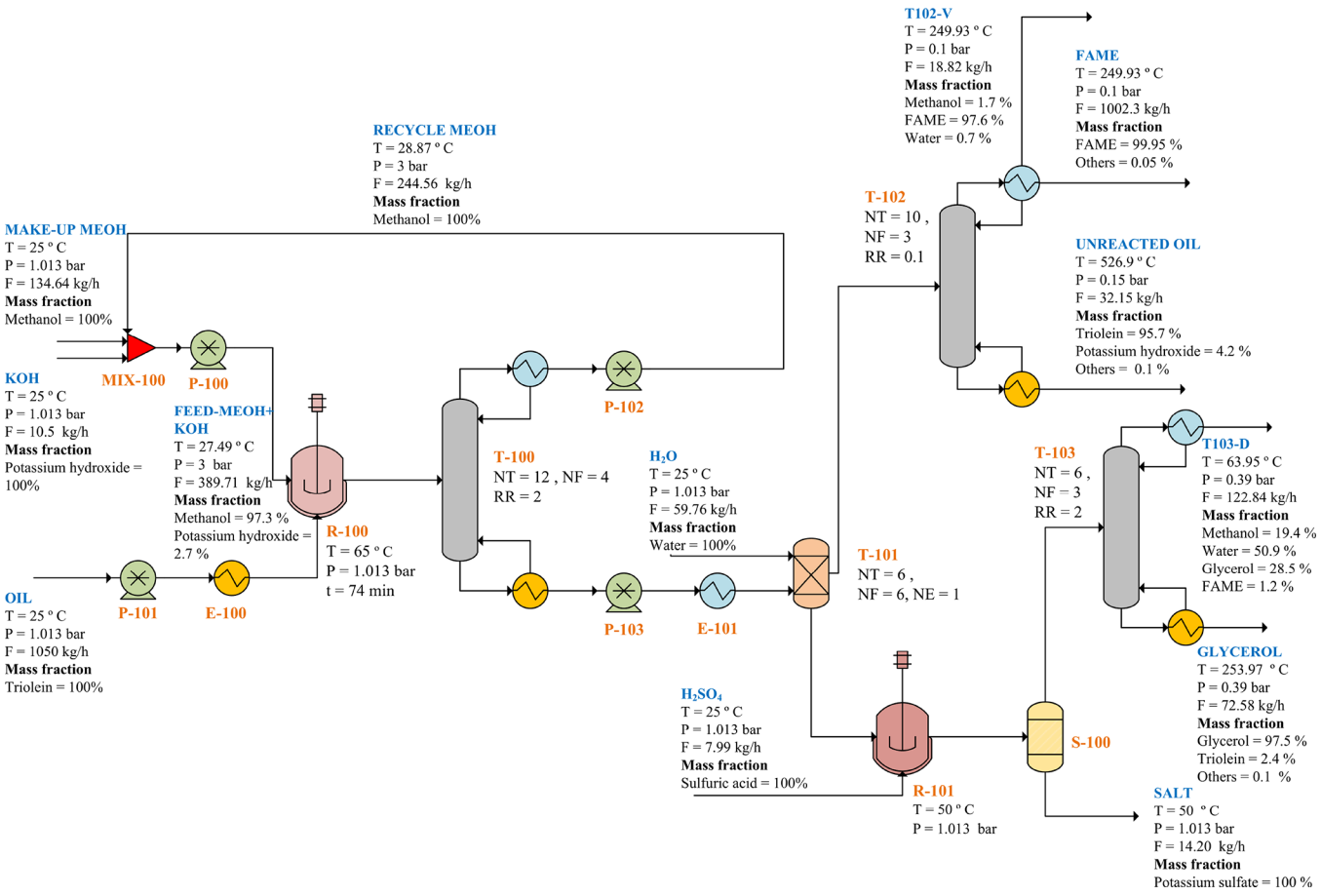

Figure 2. Simulation flowsheet of the conventional processes.

in the biodiesel yield was found with an increased catalyst concentration, suggesting that the catalyst concentration had already reached a saturation point, beyond which increasing the concentration did not improve the biodiesel yield. From the ANOVA analysis, the effect of catalyst loading and reaction time were actually insignificant.

3.4.3 Effect of the Methanol:Oil Molar Ratio and Transesterification Reaction Time on the FAME Yield. The effects of varying the methanol:oil molar ratio and reaction time on the FAME yield at a constant catalyst loading of 4 wt % were plotted in contour and surface plots (Figure 1e,f). Increasing the methanol:oil molar ratio up to 9:1 led to a significant increase in the FAME yield (Figure 1a,b), which is because higher amounts of methanol promote the reaction toward the product side. However, excessive amounts of methanol can cause the reaction to shift back toward the reactant side, leading to a decreased FAME yield. Similarly, increasing the reaction time up to 90 min increased the FAME yield (Figure 1b,c) because longer reaction times allow for greater conversion of the reactants into products. However, the FAME yield started to decrease after 90 min due to the reverse reaction.

The optimal catalyst loading level was found to be 3.27 wt % with a methanol:palm oil molar ratio of 9.98:1, reaction time of 74 min, and reaction temperature of 65 °C. Under these optimal conditions, a predicted biodiesel yield of 96.90% was obtained. To verify the accuracy of the results, the experiments were repeated three times, and the obtained yield was found to be 97.14%. Thus, the predicted values were viable and could be relied upon for future biodiesel production.

3.5 Chemical Composition of the Obtained Biodiesel. The fatty acid composition of the biodiesel produced from palm oil was determined using GC-FID. The biodiesel was composed of a variety of fatty acids, including saturated, monounsaturated, and polyunsaturated with two or three double bonds (Table S3). However, the most prominent fatty acids present were *cis*-9-octadecenoic, palmitic, and linoleic acids.

3.6 Reusability. The reusability of a catalyst is a crucial factor for its practical application in the production of biodiesel. In this study, the reusability of the 30 K/CSA catalyst was evaluated under the previously evaluated optimal reaction conditions (Section 3.4). The first reaction cycle produced a high FAME yield (97.14%) (Figure S8). However, the FAME yield decreased significantly to 85.50 and 63.50% in the second and fourth cycles, respectively. This reduction in yield may be attributed to the leaching of potassium ions from the catalyst during the recovery process.[45] Additionally, pore blockage of the catalyst active sites by reactants and products, such as triglycerides and glycerol, may have also contributed to the inhibition of catalyst activity.[49] The total basicity decreased significantly, indicating the loss of potassium compounds on the support.

From an environmental and economic standpoint, it is advantageous to use catalysts derived from renewable resources. The potential reusability and development of these catalysts may facilitate the profitable operation of the biodiesel

https://doi.org/10.1021/acsomega.3c04209
ACS Omega 2023, 8, 30598−30611

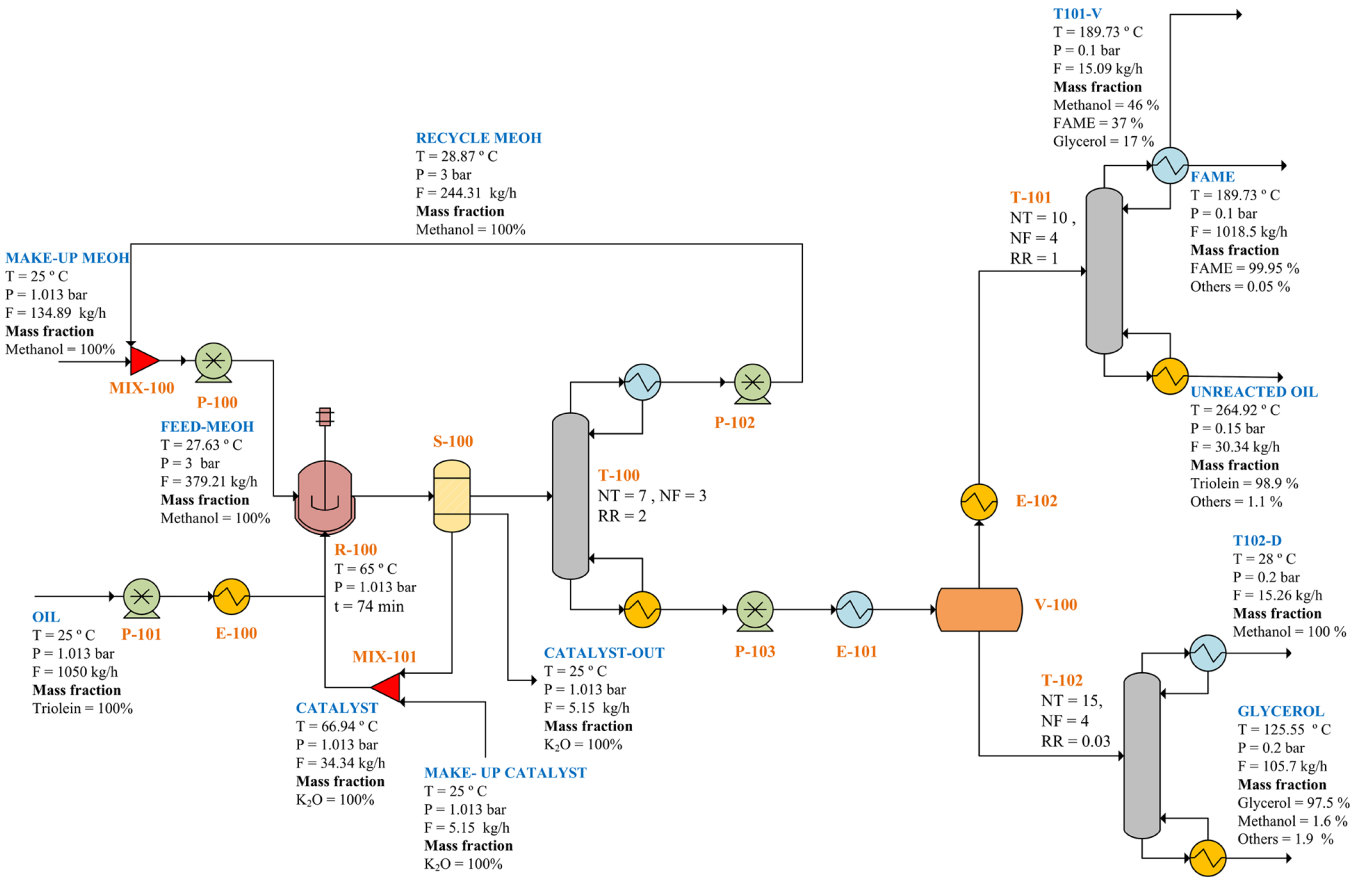

Figure 3. Simulation flowsheet of the heterogeneous catalyzed processes.

industry, as they can significantly reduce the cost of biodiesel production. For instance, the utilization of carbon or ACs as catalysts can substantially reduce the production cost. Previously, a biocatalyst impregnated with KOH for the production of biodiesel from a mixed cooking oil (sunflower and palm oils) was found to be reusable up to the fifth cycle,[1] albeit with a reduction in yield to 85.6 wt % that was attributed to the leaching of potassium ions. Similarly, in a study on the use of *Musa champa* peduncle waste ash as a catalyst for the conversion of *Jatropha curcas* oil to biodiesel, it was demonstrated that the catalyst could be reused up to three times, albeit with a yield reduction to 90.03 wt %. This decrease in yield may have been caused by the leaching of K_2CO_3.[50]

3.7 Process Analysis. *3.7.1 Conventional Process for Biodiesel Production.* The continuous process flow of conventional transesterification reaction is shown in Figure 2. The recycled and fresh top-up methanol and KOH catalyst were mixed in the mixer (M-100), while the fresh palm oil was preheated and pumped into R-100 for biodiesel production. A 96.5% conversion level of palm oil to biodiesel production is assumed. Products from R-100 are sent to the distillation column (T-100) to recover the unreacted methanol at the top and recycled into the reactor. The overhead stream contains a mixture of biodiesel, glycerol, unreacted oil, and catalyst. Because both biodiesel and glycerol have similar boiling points, the number of stages in the column was increased. Water is used as a solvent to extract glycerol from the FAME in column T-101. The raffinate phase from the extraction column flows to the vacuum distillation column (T-102) for FAME purification. The FAME is obtained as the top product, and unreacted oil is obtained as the bottom product. The remaining catalyst is neutralized by sulfuric acid, resulting in the production of potassium sulfate. The precipitated salt is removed in the solid separator (S-101). The glycerol enriched phase is purified in the distillation column (T-103). Glycerol is obtained at the bottom of the column, while water is vaporized out at the top of the column. In Figure S9, the simulation flowsheet of the conventional processes from the Aspen Plus program is represented. The mass balance and unit operations of the conventional process are shown in Tables S4 and S5.

3.7.2 Heterogeneous Catalyzed Process for Biodiesel Production. The production of biodiesel through a heterogeneous acid-catalyzed process is shown in Figure 3. The process involves mixing fresh and recycled methanol in a mixer (MIX-100), which is then pumped into reactor R-100, where it reacts with preheated palm oil in a stirred tank reactor. The solid catalyst is separated in a solid separator (S-100) and recycled back into R-100, while the liquid stream is directed to a distillation column (T-100) to recover the excess methanol. Methanol is collected as the distillate, whereas biodiesel and other components are collected at the bottom. The mixture of glycerol and biodiesel is sent to a decanter (V-100) for separation. The FAME enriched phase is directed to a multistage distillation column (T-101) for the purification of FAME under vacuum conditions. The glycerol enriched phase is directed to the distillation column (T-102) to separate glycerol at the bottom section. Figure S10 illustrates the simulation flowsheet of the heterogeneous catalyzed processes using the Aspen Plus program. The corresponding mass

https://doi.org/10.1021/acsomega.3c04209
ACS Omega 2023, 8, 30598−30611

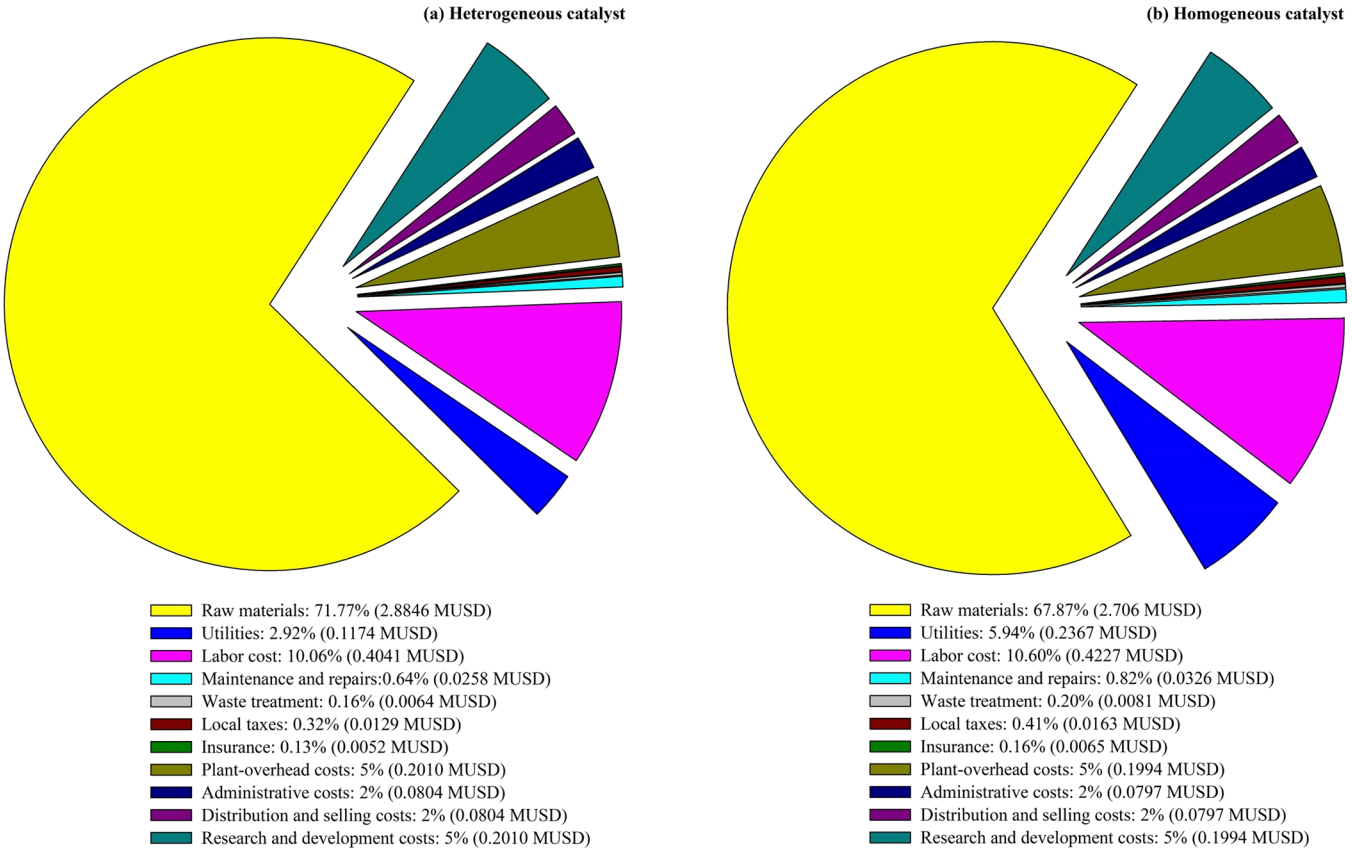

Figure 4. Total manufacturing cost (TMC) of a (a) heterogeneous and (b) conventional homogeneous catalyst.

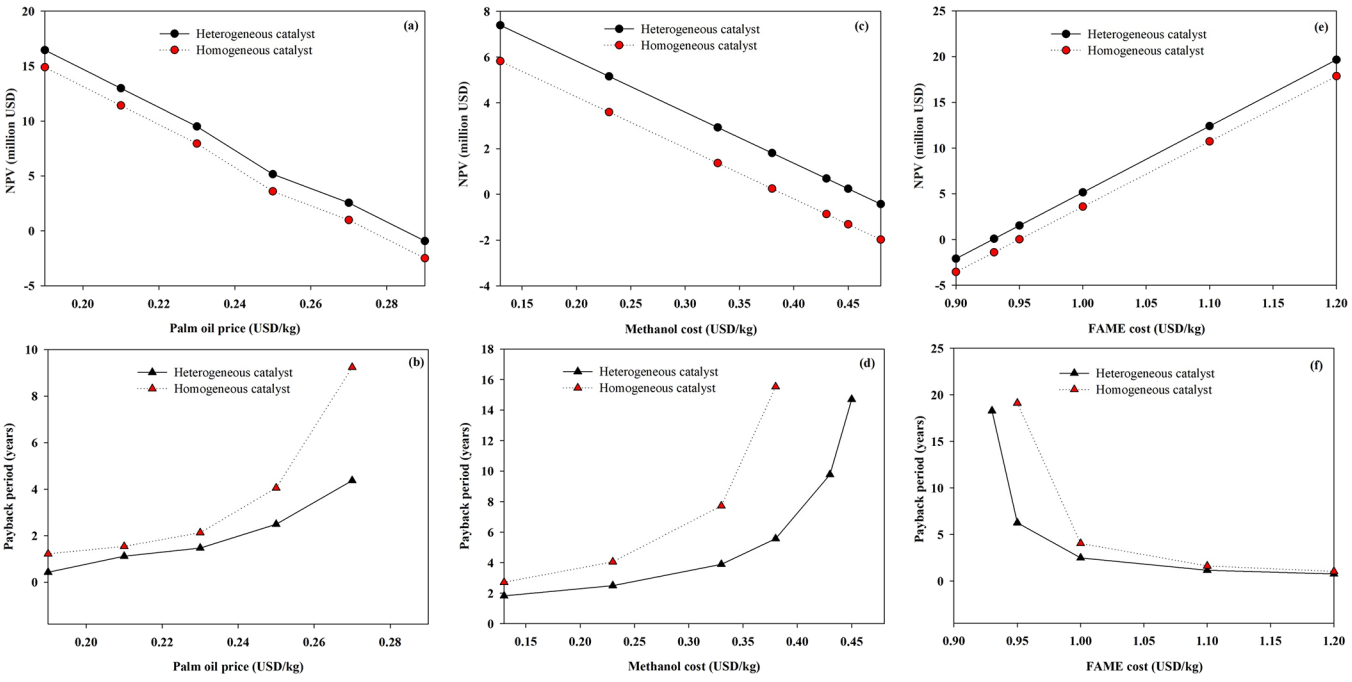

Figure 5. Sensitivity analysis of the (a, b) palm oil, (c, d) methanol, and (e, f) FAME prices.

balance and unit operations for the heterogeneous catalyzed process could be found in Tables S6 and S7.

3.8 Biodiesel Production: TEA. *3.8.1 Investment Calculation.* Considering that the cost of manufacturing (COM) is a crucial aspect of successfully operating both homogeneous and heterogeneous catalyst processes, this study provides an overview of the predetermined cost estimates in Figure 4a,b. In the heterogeneous catalyst process, the total cost was 4.02 million (M)USD, where raw materials accounted for the largest proportion at 71.77%, followed by labor costs at 10.06%. On the other hand, for the conventional process that uses homogeneous catalyst, the total cost was 3.99 MUSD,

https://doi.org/10.1021/acsomega.3c04209
ACS Omega 2023, 8, 30598−30611

with raw materials still comprising the largest portion at 67.87%, followed by labor costs at 10.60%. While the overall costs for each process were quite similar, there were notable differences in the cost breakdown.

3.8.2 Financial Performance. The profitability of a manufacturing process is crucial to determine the feasibility of a project. In this study, the financial performance of two manufacturing processes, one using a heterogeneous catalyst and the other using a homogeneous catalyst, was evaluated based on the NPV, IRR, and PBP. The heterogeneous catalyst process showed a NPV of 5.16 MUSD, an IRR of 44.2%, and a PBP of 2.49 y. In contrast, the conventional process using a homogeneous catalyst had a NPV of 3.60 MUSD, an IRR of 28.6%, and a PBP of 4.05 y. The higher NPV of the heterogeneous catalyst process compared to the conventional process using a homogeneous catalyst indicated that the former process generated more profit after considering the time value of money. Moreover, the heterogeneous catalyst process was more profitable with a higher IRR than the conventional process using a homogeneous catalyst. The shorter PBP of the heterogeneous catalyst process indicated that the initial investment would be recovered sooner compared to the conventional process using a homogeneous catalyst. Based on these financial performance results, the heterogeneous catalyst process design is a suitable and worthwhile investment.

3.8.3 Sensitivity Analysis. A key challenge in developing a sustainable process is ensuring economic viability. This study investigated the NPV and PBP of raw materials and biodiesel costs with varying prices of palm oil (0.19 to 0.29 USD/kg), methanol (0.13 to 0.48 USD/kg), and biodiesel (0.9 to 1.2 USD/kg), as represented in Figure 5. The cost of raw materials, especially palm oil and methanol, had a significant impact on the profitability of biodiesel production. As the cost of raw materials increased, the NPV decreased and the PBP lengthened. At a palm oil price of 0.29 USD/kg, the project resulted in a negative NPV and an undefined PBP. Furthermore, the use of a heterogeneous catalyst process was more profitable at lower raw materials prices compared to the conventional process using a homogeneous catalyst. In addition, the price of biodiesel also played a crucial role in the profitability of the production process, where the heterogeneous catalyst process was more sensitive to changes in the biodiesel price compared to the conventional process using a homogeneous catalyst.

3.9 Environmental Assessment. The carbon emissions from biodiesel production processes are mainly generated from the consumption of electricity and steam. This study compared the carbon footprint of the conventional and the heterogeneous catalyzed processes. The conventional process had a higher CO_2 emission (1784.62 ton/y) compared to the heterogeneous catalyzed process (1401.86 ton/y). The high carbon emissions from the conventional process were due to the significant energy requirement for neutralization and glycerol-biodiesel separation processes.

4. CONCLUSIONS

The study demonstrated the potential of the CSA-supported K_2CO_3 catalyst in producing biodiesel from palm oil and methanol. The optimized reaction conditions of a methanol:oil molar ratio of 9.98:1, catalyst loading of 3.27 wt %, reaction time of 74 min, and a reaction temperature of 65 °C gave a high obtained biodiesel yield of 97.14%. Furthermore, the methanol:oil molar ratio was found to be the most significant factor affecting the yield. The reliability of the model for predicting the biodiesel yield was confirmed by the high R^2 (0.9431) and adj. R^2 (0.8920) values. Furthermore, the TEA showed that the heterogeneous catalyst process had a higher NPV and IRR and shorter PBP compared to the conventional process. Promoting the adoption of a heterogeneous catalyst process is advocated due to the substantial influence of raw material expenses on the profitability of biodiesel production. This process not only mitigates costs but also exhibits enhanced environmental compatibility, heightened biodiesel productivity, and augmented profitability.

■ ASSOCIATED CONTENT

Supporting Information

The Supporting Information is available free of charge at https://pubs.acs.org/doi/10.1021/acsomega.3c04209.

Experimental factors and levels used in the RSM-CCD analysis of biodiesel synthesis; basic strength and total basicity of the prepared catalysts; fatty acid methyl ester composition of the biodiesel synthesized from palm oil and methanol using the 30 K/CSA catalyst; mass balance of the conventional processes; mass balance of the heterogeneous catalyzed processes; unit operation of the conventional processes; unit operation of the heterogeneous catalyzed processes; XRD patterns of the CSA support and the 25 K/CSA, 30 K/CSA, and 35 K/CSA catalysts; FTIR spectrum of the CSA and 30 K/CSA catalysts; SEM images of the CSA support and 30 K/CSA catalyst; EDS images of the CSA support and 30 K/CSA catalyst; XPS spectra, as wide and narrow scan mode of the CSA support and 30 K/CSA catalyst; comparison graph between the predicted and actual FAME value and diagnostic plots for the obtained second order polynomial model obtained from the RSM-CCD analysis; perturbation plot on FAME yield; reusability studies of the 30 K/CSA catalyst; simulation flowsheet of the conventional processes; and simulation flowsheet of the heterogeneous catalyzed processes (PDF)

■ AUTHOR INFORMATION

Corresponding Author

Jakkrapong Jitjamnong − *Petroleum Technology Program, Industrial Technology Department, Faculty of Industrial Education and Technology, Rajamangala University of Technology Srivijaya, Songkhla 90000, Thailand;* orcid.org/0000-0002-8628-3616; Phone: +66 85 921 9559; Email: jakkrapong.j@rmutsv.ac.th; Fax: +66 7 4317178

Authors

Phonsan Saetiao − *Petroleum Technology Program, Industrial Technology Department, Faculty of Industrial Education and Technology, Rajamangala University of Technology Srivijaya, Songkhla 90000, Thailand*

Napaphat Kongrit − *Petroleum Technology Program, Industrial Technology Department, Faculty of Industrial Education and Technology, Rajamangala University of Technology Srivijaya, Songkhla 90000, Thailand*

https://doi.org/10.1021/acsomega.3c04209
ACS Omega 2023, 8, 30598−30611

Chatrawee Direksilp − *Institute of functional interfaces (IFG), Karlsruhe Institute of Technology (KIT), Karlsruhe, Eggenstein-Leopoldshafen 76344, Germany*

Chin Kui Cheng − *Center for Catalysis and Separation, Department of Chemical Engineering, College of Engineering, Khalifa University of Science and Technology, 127788 Abu Dhabi, United Arab Emirates;* orcid.org/0000-0002-2984-7606

Nonlapan Khantikulanon − *Department of Environmental Health, Faculty of Public Health, Valaya Alongkorn Rajabhat University under The Royal Patronage, Pathum Thani 10120, Thailand*

Complete contact information is available at: https://pubs.acs.org/10.1021/acsomega.3c04209

Notes

The authors declare no competing financial interest.

■ ACKNOWLEDGMENTS

The authors express their gratitude to the Rajamangala University of Technology Srivijaya, Songkhla, Thailand, for their valuable contributions to this research.

■ REFERENCES

(1) Dharmalingam, B.; Balamurugan, S.; Wetwatana, U.; Tongnan, V.; Sekhar, C.; Paramasivam, B.; Cheenkachorn, K.; Tawai, A.; Sriariyanun, M. Comparison of Neural Network and Response Surface Methodology Techniques on Optimization of Biodiesel Production from Mixed Waste Cooking Oil Using Heterogeneous Biocatalyst. *Fuel* **2023**, *340*, No. 127503.

(2) Sangeetha, B.; Priya, S. M.; Pravin, R.; Tamilarasan, K.; Baskar, G. Process Optimization and Technoeconomic Assessment of Biodiesel Production by One-Pot Transesterification of Ricinus Communis Seed Oil. *Bioresour. Technol.* **2023**, *376*, No. 128880.

(3) Karkal, S. S.; Rathod, D. R.; Jamadar, A. S.; Mamatha, S. S.; Kudre, T. G. Production Optimization, Scale-up, and Characterization of Biodiesel from Marine Fishmeal Plant Oil Using Portunus Sanguinolentus Crab Shell Derived Heterogeneous Catalyst. *Biocatal. Agric. Biotechnol.* **2023**, *47*, No. 102571.

(4) Masera, K.; Hossain, A. K. Advancement of Biodiesel Fuel Quality and NOx Emission Control Techniques. *Renewable Sustainable Energy Rev.* **2023**, *178*, No. 113235.

(5) Rodríguez-Guerrero, J. K.; Rubens, M. F.; Rosa, P. T. V. Production of Biodiesel from Castor Oil Using Sub and Supercritical Ethanol: Effect of Sodium Hydroxide on the Ethyl Ester Production. *J. Supercrit. Fluids* **2013**, *83*, 124−132.

(6) Almasi, S.; Najafi, G.; Ghobadian, B.; Jalili, S. Biodiesel Production from Sour Cherry Kernel Oil as Novel Feedstock Using Potassium Hydroxide Catalyst: Optimization Using Response Surface Methodology. *Biocatal. Agric. Biotechnol.* **2021**, *35*, No. 102089.

(7) Brahma, S.; Basumatary, B.; Basumatary, S. F.; Das, B.; Brahma, S.; Rokhum, S. L.; Basumatary, S. Biodiesel Production from Quinary Oil Mixture Using Highly Efficient Musa Chinensis Based Heterogeneous Catalyst. *Fuel* **2023**, *336*, No. 127150.

(8) Bahadorizadeh, O.; Sobati, M. A.; Shahnazari, S. Emission Characteristics of a Semi-Industrial Boiler Fueled by Waste Cooking Oil Biodiesel Containing Different Metal Oxide Nanoparticles. *Process Saf. Environ. Prot.* **2022**, *158*, 199−209.

(9) Yusuff, A. S.; Gbadamosi, A. O.; Atray, N. Development of a Zeolite Supported CaO Derived from Chicken Eggshell as Active Base Catalyst for Used Cooking Oil Biodiesel Production. *Renewable Energy* **2022**, *197*, 1151−1162.

(10) Shibasaki-Kitakawa, N.; Hiromori, K.; Ihara, T.; Nakashima, K.; Yonemoto, T. Production of High Quality Biodiesel from Waste Acid Oil Obtained during Edible Oil Refining Using Ion-Exchange Resin Catalysts. *Fuel* **2015**, *139*, 11−17.

(11) Maleki, B.; Singh, B.; Eamaeili, H.; Venkatesh, Y. K.; Talesh, S. S. A.; Seetharaman, S. Transesterification of Waste Cooking Oil to Biodiesel by Walnut Shell/Sawdust as a Novel, Low-Cost and Green Heterogeneous Catalyst: Optimization via RSM and ANN. *Ind. Crops Prod.* **2023**, *193*, No. 116261.

(12) Dougher, M.; Soh, L.; Bala, A. M. Techno-Economic Analysis of Interesterification for Biodiesel Production. *Energy & Fuels* **2023**, *37*, 2912−2925.

(13) Yameen, M. Z.; AlMohamadi, H.; Naqvi, S. R.; Noor, T.; Chen, W.-H.; Amin, N. A. S. Advances in Production & Activation of Marine Macroalgae-Derived Biochar Catalyst for Sustainable Biodiesel Production. *Fuel* **2023**, *337*, No. 127215.

(14) Hervy, M.; Berhanu, S.; Weiss-Hortala, E.; Chesnaud, A.; Gérente, C.; Villot, A.; Minh, D. P.; Thorel, A.; Le Coq, L.; Nzihou, A. Multi-Scale Characterisation of Chars Mineral Species for Tar Cracking. *Fuel* **2017**, *189*, 88−97.

(15) Foroutan, R.; Mohammadi, R.; Razeghi, J.; Ramavandi, B. Biodiesel Production from Edible Oils Using Algal Biochar/CaO/K_2CO_3 as a Heterogeneous and Recyclable Catalyst. *Renewable Energy* **2021**, *168*, 1207−1216.

(16) Naveenkumar, R.; Baskar, G. Process Optimization, Green Chemistry Balance and Technoeconomic Analysis of Biodiesel Production from Castor Oil Using Heterogeneous Nanocatalyst. *Bioresour. Technol.* **2021**, *320*, No. 124347.

(17) Ravichandran, P.; Rajendran, N.; Al-Ghanim, K. A.; Govindarajan, M.; Gurunathan, B. Investigations on Evaluation of Marine Macroalgae Dictyota Bartayresiana Oil for Industrial Scale Production of Biodiesel through Technoeconomic Analysis. *Bioresour. Technol.* **2023**, *374*, No. 128769.

(18) Kongrit, N.; Chanakaewsomboon, I.; Jitjamnong, J.; Luengnaruemitchai, A.; Kasetsomboon, N.; Chuaykarn, N.; Direksilp, C.; Khantikulanon, N.; Cheng, C. K. Development of Mangosteen Peel Ash as a Heterogeneous Catalyst for Palm Oil-Derived Fatty Acid Methyl Ester Production. *Agric. Nat. Resour.* **2022**, *56*, 957−970.

(19) Jitjamnong, J.; Thunyaratchatanon, C.; Luengnaruemitchai, A.; Kongrit, N.; Kasetsomboon, N.; Sopajarn, A.; Chuaykarn, N.; Khantikulanon, N. Response Surface Optimization of Biodiesel Synthesis over a Novel Biochar-Based Heterogeneous Catalyst from Cultivated (Musa Sapientum) Banana Peels. *Biomass Convers. Biorefin.* **2021**, *11*, 2795−2811.

(20) Albuquerque, A. A.; Ng, F. T. T.; Danielski, L.; Stragevitch, L. Phase Equilibrium Modeling in Biodiesel Production by Reactive Distillation. *Fuel* **2020**, *271*, No. 117688.

(21) Li, R. Integrating the Composition of Food Waste into the Techno-Economic Analysis of Waste Biorefineries for Biodiesel Production. *Bioresour. Technol. Rep.* **2022**, *20*, No. 101254.

(22) Ng, W. Z.; Obon, A. A.; Lee, C. L.; Ong, Y. H.; Gourich, W.; Maran, K.; Tang, D. B. Y.; Song, C. P.; Chan, E.-S. Techno-Economic Analysis of Enzymatic Biodiesel Co-Produced in Palm Oil Mills from Sludge Palm Oil for Improving Renewable Energy Access in Rural Areas. *Energy* **2022**, *243*, No. 122745.

(23) Gengiah, K.; Gurunathan, B.; Rajendran, N.; Han, J. Process Evaluation and Techno-Economic Analysis of Biodiesel Production from Marine Macroalgae Codium Tomentosum. *Bioresour. Technol.* **2022**, *351*, No. 126969.

(24) Chuenphan, T.; Yurata, T.; Sema, T.; Chalermsinsuwan, B. Techno-Economic Sensitivity Analysis for Optimization of Carbon Dioxide Capture Process by Potassium Carbonate Solution. *Energy* **2022**, *254*, No. 124290.

(25) Sultana, A. I.; Reza, M. T. Techno-Economic Assessment of Superactivated Hydrochar Production by KOH Impregnation Compared to Direct Chemical Activation. *Biomass Convers. Biorefin.* **2022**, 1.

(26) Tiwari, A. K.; Somwanshi, A. Techno-Economic Analysis of Mini Solar Distillation Plants Integrated with Reservoir of Garden Fountain for Hot and Dry Climate of Jodhpur (India). *Sol. Energy* **2018**, *160*, 216−224.

(27) Hamed, S. M.; El Shimi, H. I.; van Dijk, J. R.; Osman, A. I.; Korany, S. M.; AbdElgawad, H. A Novel Integrated System for Heavy Metals Removal and Biodiesel Production via Green Microalgae: A Techno-Economic Feasibility Assessment. *J. Environ. Chem. Eng.* **2022**, *10*, No. 108804.
(28) Gade, S. M.; Saptal, V. B.; Bhanage, B. M. Perception of Glycerol Carbonate as Green Chemical: Synthesis and Applications. *Catal. Commun.* **2022**, *172*, No. 106542.
(29) Yu, B.-Y.; Wu, P.-J.; Tsai, C.-C.; Lin, S.-T. Evaluating the Direct CO_2 to Diethyl Carbonate (DEC) Process: Rigorous Simulation, Techno-Economical and Environmental Evaluation. *J. CO2 Util.* **2020**, *41*, No. 101254.
(30) Turton, R.; Bailie, R. C.; Whiting, W. B.; Shaeiwitz, J. A.; Bhattacharyya, D. *Analysis, Synthesis, and Design of Chemical Processes*, 4th ed.; Prentice Hall: Upper Saddle River, New Jersey, 2013.
(31) Zhou, X.; Li, S.; Wang, Y.; Zhang, J.; Zhang, Z.; Wu, C.; Chen, X.; Feng, X.; Liu, Y.; Zhao, H.; Yan, H.; Yang, C. Crude oil hierarchical catalytic cracking for maximizing chemicals production: Pilot-scale test, process optimization strategy, techno-economic-society-environment assessment. *Energy Convers. Manage.* **2022**, *253*, No. 115149.
(32) Zhou, X.; Sun, Z.; Yan, H.; Feng, X.; Zhao, H.; Liu, Y.; Chen, X.; Yang, C. Produce petrochemicals directly from crude oil catalytic cracking, a techno-economic analysis and life cycle society-environment assessment. *J. Cleaner Prod.* **2021**, *308*, No. 127283.
(33) Zhou, X.; Yan, H.; Sun, Z.; Feng, X.; Zhao, H.; Liu, Y.; Chen, X.; Yang, C. Opportunities for utilizing waste cooking oil in crude to petrochemical process: Novel process design, optimal strategy, techno-economic analysis and life cycle society-environment assessment. *Energy* **2021**, *237*, No. 121530.
(34) Peters, M. S.; Timmerhaus, K. D.; West, R. E. *Plant Design and Economics for Chemical Engineers*, 5th ed.; McGraw-Hill chemical engineering series; McGraw-Hill: New York, 2003.
(35) Mustafa, A.; Niikura, F.; Pastore, C.; Allam, H. A.; Hassan, O. B.; Mustafa, M.; Inayat, A.; Salah, S. A.; Salam, A. A.; Mohsen, R. Selective Synthesis of Alpha Monoglycerides by a Clean Method: Techno-Economic and Environmental Assessment. *Sustainable Chem. Pharm.* **2022**, *27*, No. 100690.
(36) Zhao, C.; Lv, P.; Yang, L.; Xing, S.; Luo, W.; Wang, Z. Biodiesel Synthesis over Biochar-Based Catalyst from Biomass Waste Pomelo Peel. *Energy Convers. Manage.* **2018**, *160*, 477−485.
(37) Balajii, M.; Niju, S. Banana Peduncle − A Green and Renewable Heterogeneous Base Catalyst for Biodiesel Production from Ceiba Pentandra Oil. *Renewable Energy* **2020**, *146*, 2255−2269.
(38) Liu, H.; Su, L.; Liu, F.; Li, C.; Solomon, U. U. Cinder Supported K_2CO_3 as Catalyst for Biodiesel Production. *Appl. Catal., B: Environ.* **2011**, *106*, 550−558.
(39) Gohain, M.; Devi, A.; Deka, D. Musa Balbisiana Colla Peel as Highly Effective Renewable Heterogeneous Base Catalyst for Biodiesel Production. *Ind. Crops Prod.* **2017**, *109*, 8−18.
(40) Daimary, N.; Eldiehy, K. S. H.; Boruah, P.; Deka, D.; Bora, U.; Kakati, B. K. Potato Peels as a Sustainable Source for Biochar, Bio-Oil and a Green Heterogeneous Catalyst for Biodiesel Production. *J. Environ. Chem. Eng.* **2022**, *10*, No. 107108.
(41) Sharma, M.; Khan, A. A.; Puri, S. K.; Tuli, D. K. Wood Ash as a Potential Heterogeneous Catalyst for Biodiesel Synthesis. *Biomass Bioenergy* **2012**, *41*, 94−106.
(42) Li, X.; Zuo, Y.; Zhang, Y.; Fu, Y.; Guo, Q. In Situ Preparation of K_2CO_3 Supported Kraft Lignin Activated Carbon as Solid Base Catalyst for Biodiesel Production. *Fuel* **2013**, *113*, 435−442.
(43) Gouda, S. P.; Ngaosuwan, K.; Assabumrungrat, S.; Selvaraj, M.; Halder, G.; Rokhum, S. L. Microwave Assisted Biodiesel Production Using Sulfonic Acid-Functionalized Metal-Organic Frameworks UiO-66 as a Heterogeneous Catalyst. *Renewable Energy* **2022**, *197*, 161−169.
(44) Sharma, A.; Kodgire, P.; Kachhwaha, S. S. Investigation of Ultrasound-Assisted KOH and CaO Catalyzed Transesterification for Biodiesel Production from Waste Cotton-Seed Cooking Oil: Process Optimization and Conversion Rate Evaluation. *J. Cleaner Prod.* **2020**, *259*, No. 120982.
(45) Falowo, O. A.; Oloko-Oba, M. I.; Betiku, E. Biodiesel Production Intensification via Microwave Irradiation-Assisted Transesterification of Oil Blend Using Nanoparticles from Elephant-Ear Tree Pod Husk as a Base Heterogeneous Catalyst. *Chem. Eng. Process.* **2019**, *140*, 157−170.
(46) Ibrahim, A. P.; Omilakin, R. O.; Betiku, E. Optimization of Microwave-Assisted Solvent Extraction of Non-Edible Sandbox (Hura Crepitans) Seed Oil: A Potential Biodiesel Feedstock. *Renewable Energy* **2019**, *141*, 349−358.
(47) Basumatary, B.; Basumatary, S.; Das, B.; Nath, B.; Kalita, P. Waste Musa Paradisiaca Plant: An Efficient Heterogeneous Base Catalyst for Fast Production of Biodiesel. *J. Cleaner Prod.* **2021**, *305*, No. 127089.
(48) Betiku, E.; Okeleye, A. A.; Ishola, N. B.; Osunleke, A. S.; Ojumu, T. V. Development of a Novel Mesoporous Biocatalyst Derived from Kola Nut Pod Husk for Conversion of Kariya Seed Oil to Methyl Esters: A Case of Synthesis, Modeling and Optimization Studies. *Catal. Lett.* **2019**, *149*, 1772−1787.
(49) Daimary, N.; Eldiehy, K. S. H.; Bora, N.; Boruah, P.; Rather, M. A.; Mandal, M.; Bora, U.; Deka, D. Towards Integrated Sustainable Biofuel and Chemical Production: An Application of Banana Pseudostem Ash in the Production of Biodiesel and Recovery of Lignin from Bamboo Leaves. *Chemosphere* **2023**, *314*, No. 137625.
(50) Nath, B.; Basumatary, B.; Brahma, S.; Das, B.; Kalita, P.; Rokhum, S. L.; Basumatary, S. Musa Champa Peduncle Waste-Derived Efficient Catalyst: Studies of Biodiesel Synthesis, Reaction Kinetics and Thermodynamics. *Energy* **2023**, *270*, No. 126976.

https://doi.org/10.1021/acsomega.3c04209
ACS Omega 2023, 8, 30598−30611